2008 IEEE International Conference on
Robotics and Automation
Pasadena, CA, USA, May 19-23, 2008

Geometric Design of the LineScout, a Teleoperated Robot for Power Line Inspection and Maintenance

Nicolas Pouliot and Serge Montambault, Hydro-Québec

Abstract – Power line inspection and maintenance are fields of application where robotics has yet to be introduced. However, as in many other hostile environments, substantial benefits in terms of workers safety and quality of inspection results could arise. This paper describes one of the latest initiatives toward that goal by presenting the design of a teleoperated robot called the "LineScout". This moving platform has the capacity to cross obstacles found on the line. Special care was taken early in the design phase to account for the context of power utility operation and to customize the geometric parameters to the specific features of the electric power network. The final prototype incorporates several key mechanical design features, which are briefly described. The LineScout is now validated, fully tested and ready to undertake pilot projects.

***Index terms*—Mechanical design, field robotics, telerobotics.**

I. Introduction

Working on energized power lines is now a necessity for most transmission grid owners. For inspection and maintenance activity, innovation is seek as transmission networks are pressured by increasing loads and high reliability requirements [1-2].

Although some tasks have been successfully automated [3-4] and more research teams have been active in mobile robotics in recent years [5-7], most research results published in the past cover analysis or prototype technologies that never made it onto transmission networks [8-9]. An extensive review of these technologies was presented in [10].

Hydro-Québec undertook a research program aimed at developing robotic technologies to perform inspection and maintenance on its transmission line network. Valuable and encouraging field results where obtained with a compact and simple technology called the "LineROVer"[10]. The next logical step was to develop a new platform capable not only of carrying different types of sensors for inspection and maintenance but also of crossing the various obstacles found on power lines, including the ones encountered on bundle of conductors. This research effort resulted in a teleoperated robot named the "LineScout", whose specifications were first presented to the power line community in late 2006 [11]. Reference [12] showed the LineScout in a field-oriented perspective, describing the integration of mechanical and electrical systems and the validation performed to verify its reliability.

This paper describes for the first time the geometrical constraints that were followed and emphasizes decisive analyses performed early in the project. The assumption is that strategic decisions based on these analyses were critical for robot versatility and its acceptance within the end-user community. Section II presents the operational context inherent to power utilities that was considered upfront, in order to maximize the chance of successful implementation. Section III presents the approach selected and its advantages. Section IV gives insights on the analyses performed at the geometric design stage to customize the approach to the types and sequence of obstacles found on the Hydro-Québec network. Section V presents some key design features of the platform while Section VI concludes and opens on future developments.

II. Power Utility Context and Needs

A. Types and Sequences of Obstacles

A general schematic of an overhead transmission line is presented in Fig. 1.

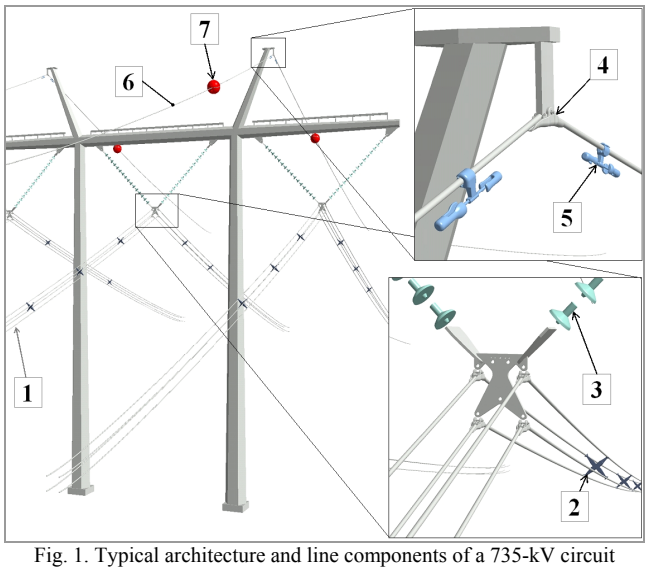

Fig. 1. Typical architecture and line components of a 735-kV circuit

The highest voltage lines (735-765 kV) found on the Hydro-Québec transmission system are in a four-conductor bundle configuration (1). Along the bundle, spacer dampers (2) are installed every 60 m to maintain the prescribed distance between conductors. Bundles of two conductors and single conductors are used for lower voltages.

Conductors are suspended from towers by means of insulators strings (3), connected with a suspension clamp (4). Vibration dampers (5), installed near towers, are found

in many shapes and sizes, and can also be found in groups of two or three. An overhead ground wire (OGW) (6) is suspended on the top of the steel structure, essentially acting as protection against lightning strikes. On river and highway crossings, warning spheres (7) are installed on OGWs as markers for planes and helicopters.

Numerous other types of obstacles can be found on a given network. The 0.76-m warning sphere (Fig. 2-A) was identified as the longest obstacle commonly found on the network. This length encompasses other types of relatively long obstacles, such as double-suspension clamps (Fig. 2B) and corona-ring suspension clamps (Fig. 2C). Components can have slipped or break (Fig. 2-D). More important, obstacles occur in sequences with only a certain (short) distance that separates one obstacle from the next (Fig. 2-E). This distance is not specific to the type of obstacle but varies within a certain range, based on span length, tower type, etc.

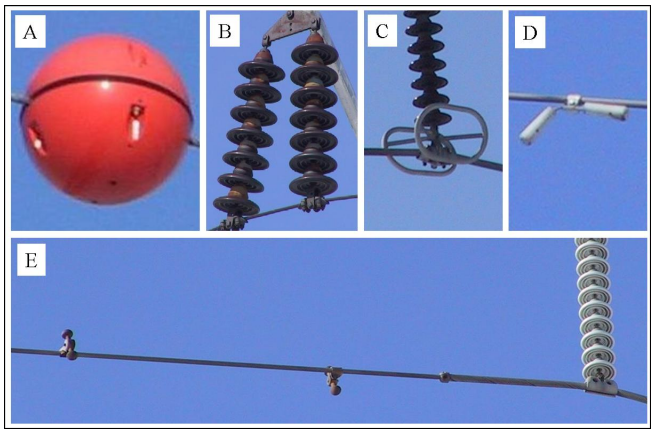

Fig. 2. Different types of obstacles

B. *Types of Tasks*

Three categories of tasks are being considered for the LineScout. The first and probably most useful is visual inspection. This does not entail contacting components but only pointing a camera at the area of interest. Being on the conductor provides a stable, nearby vantage point, valuable to assess the condition of components such as hardware, dampers, ceramic insulators, etc. Secondly, commercial sensors exist for line inspection and they are meant to be held on insulated sticks by linemen. The LineScout is an alternative means to bring these sensors to the line and safely operate them. Lastly, new applications that entail contacting components may be proposed and developed internally, such as a clamping device installed for temporary repair of broken strands. Consequently, the potential for a more refined type of control must be provided.

C. *Type of Control*

Linemen's expertise is essential to assure the quality of inspection and is a critical asset to maintain within an organization. The purpose of the technology is to extend the reach of the lineman's arm and eyes. For that reason, teleoperation control must be preferred over autonomous robots. However, the design challenge resides in providing a tool that is intuitive to control, is safe for the network and has the potential to become more autonomous as it matures.

D. *Design Requirements*

Since inspection must be performed on energized lines, one of the most important requirements, besides being robust to electromagnetic interference (EMI), is to minimize the size and weight of the platform so that a safe dielectric distance from ground and other circuits is maintained. Table 1 summarizes various constraints and target values.

TABLE 1
LINESCOUT TECHNICAL SPECIFICATIONS

Specification	Value
Line components and environment	
Conductor diameter	12 – 60 mm
Splice diameter	25 – 85 mm
Maximum obstacle length	0.84 m
Maximum conductor temperature	95.0°C
Number of conductors	1 – 4
Maximum slope in span	25°
Ambient operating temperature	0°C – 40°C
Platform	
Weight	100 kg
Length x Height	1.40 m x 0.75 m
Traction force	500 N
Linear speed	1.0 m/s
Battery life	5.0 – 8.0 hours
Communication signal range	5.0 km
EMI robustness (up to)	735 kV – 1000 A

III. APPROACH AND CONCEPTUAL DESIGN

A. *Crossing Principle*

The LineScout's usual means of travel is to roll on two wheels supported by the conductor (or OGW). This allows it to move quickly and efficiently as well as to roll over some obstacles (e.g., compression splices and vibration dampers). As schematized in Fig. 3, the LineScout is built around three independent frames. The wheel frame (in blue) includes two motorized rubber wheels serving as traction wheels. The arm frame (in white) supports two arms and two grippers. Finally, the center frame (white circle) links the first two frames together and allows them to slide and rotate.

In step 1, the LineScout stops in front of the obstacle to cross. Between the traction wheels but very close to them are two sets of safety rollers (shown by small rectangles), which clamp firmly onto the conductors from below to secure the vehicle.

In step 2, the arm frame and center frame slide forward and rotate slightly so that the two grippers are now located on either side of the obstacle.

Step 3 shows the platform configuration after a series of movements. First, the arms have risen up to the conductor and the grippers clamped onto it, providing a new set of supports for the vehicle. Then, the safety rollers have

opened and a mechanism has folded down the traction wheels below the conductor (or OGW). Finally, the wheel frame and the center frame have crossed to the opposite side by again sliding and rotating beneath the obstacle.

In step 4, the mechanism unfolds to bring the traction wheels back onto the conductor, allowing the safety rollers to secure their grasp again so the grippers can be opened safely. The arms then return to their initial lowered position. Once the arm frame and center frame are brought back to the middle position, the vehicle is ready to continue rolling down the line.

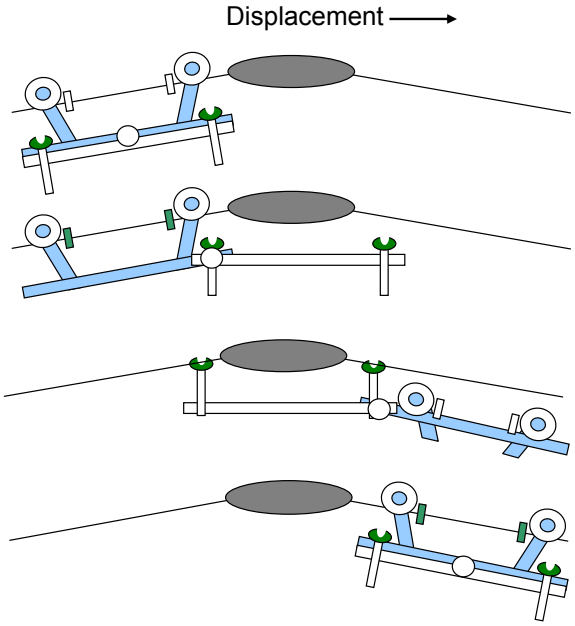

Fig. 3. Obstacle-clearing sequence

B. *Advantages of the Proposed Mechanism*

The chosen approach is conceptually very simple since it entails a single grasp on both sides of the obstacle, and a single-step transfer of the wheeled part of the robot. Most of the vehicle structure is located beneath the conductor, in an area that is generally obstacle-free. The advantages below also apply.

1) Moving Center of Rotation

One key feature of the approach is that the center of rotation actually *translates* with the center frame. Achieving this design challenge minimizes the length of translation rails required by splitting them equally between the wheel frame and arm frame. The solution is also more compact since the two moving frames tend to follow more closely the natural shape of the conductor suspended at the supporting tower.

2) Moving Center of Gravity

Since the center frame supports a fair fraction of the overall weight (e.g., onboard electronics and battery), the LineScout's overall center of gravity always remains either between or very close to the supporting elements (wheels or grippers). This minimizes cantilevered distances, reducing the size of the structure required. The center of gravity is thus always located lower than the conductor, assuring stable behavior under side loads such as strong wind.

3) Wheelbase

Because of the large translation capacity, the taken approach allows the LineScout's wheelbase to be almost as long as its overall length. This preserves the stability in steep slopes as the weight transfer from one wheel to the other is minimized. Furthermore, such a long wheelbase is needed to support significantly heavier payload, such as inspection tools, sensors or extra cameras. This LineScout's key feature is novel when compared to most past power line inspection prototypes.

4) Redundancy

As long as there is no horizontal deviation at the supporting tower, the geometric problem of grasping the conductor with each gripper is planar and thus, theoretically, requires only two degrees of freedom (DOFs). Since the length of both arms can be adjusted independently, the rotational DOF may be viewed as redundant. This redundancy is available for extra adjustments, giving the operator greater leeway in controlling the LineScout.

IV. Geometric Design

A. *Nomenclature and Conventions*

This section deals with the geometric analysis whereby the approach was customized for the series of obstacles found on the local network, identified through an extensive survey and several visits to field installations. Tables 2 to 4, illustrated by Fig. 4 to Fig. 6, present the nomenclature used.

TABLE 2
WHEEL-FRAME GEOMETRIC PARAMETERS

Geometric parameter	Symbol
Half-wheelbase of the traction wheels	E_W
Half-wheelbase of the safety rollers	E_R
External diameter of the traction wheels	D_W
Width of safety roller modules	D_R
Distance from conductor to the axis of translation	L_C
Distance from conductor to center of mass ($\mathbf{p_W}$)	L_W
Mass of the Wheel Frame	M_W
Absolute angle of the Wheel frame	θ_W

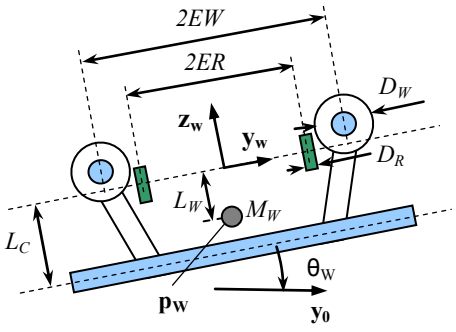

Fig. 4. Wheel-Frame Nomenclature

In Fig. 4, reference axis W ($\mathbf{F_W}$) is attached to the wheel frame halfway between the two Traction Wheels with axis $\mathbf{z_W}$, pointing up, considered as a symmetry axis. $\mathbf{y_W}$ conventionally points toward the right of the schematic. In a similar manner, reference axis G ($\mathbf{F_G}$) is attached to the gripper frame (Fig. 5), halfway between the grippers and at the same distance L_C from the axis of translation.

TABLE 3
GRIPPER FRAME GEOMETRIC PARAMETERS

Geometric parameter	Symbol
Half-wheelbase of the grippers	E_G
Width of gripper modules	D_G
Distance from conductor to the axis of translation	L_C
Distance from conductor to center of mass ($\mathbf{p}_G$)	L_G
Mass of the gripper frame	M_G
Absolute angle of the gripper frame	θ_G

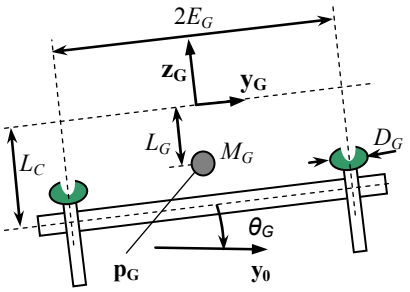

Fig. 5. Gripper-Frame Nomenclature

Note that on Fig. 6, which represents the complete assembly of the three frames, reference axis C ($\mathbf{F_C}$) is attached to the Center Frame and aligned with axis $\mathbf{F_G}$. In other words, while the linear translation measuring t occurs simultaneously and symmetrically between $\mathbf{F_W}$ and $\mathbf{F_C}$ on the one hand, and between $\mathbf{F_C}$ and $\mathbf{F_G}$ on the other hand, the rotation θ_C actually occurs only between $\mathbf{F_W}$ and $\mathbf{F_C}$. Also note that the first supporting elements (wheel $\mathbf{w_1}$, roller $\mathbf{r_1}$ and gripper $\mathbf{g_1}$) are on the positive side of their respective **y**-axis.

TABLE 4
ASSEMBLED LINESCOUT GEOMETRIC PARAMETERS

Geometric parameter	Symbol
Wheel contact point coordinates on conductor	$\mathbf{w}_{1,2}$
Roller contact point coordinates on conductor	$\mathbf{r}_{1,2}$
Gripper contact point coordinates on conductor	$\mathbf{g}_{1,2}$
Change of slope point coordinates or summit	**s**
Change of slope from one side to the next at summit	θ_S
Distance from wheel frame to the summit (upward)	L_{SU}
Distance from the summit to gripper #1 (downward)	L_{SD}
Gripper excursion required to reach the conductor	$h_{1,2}$

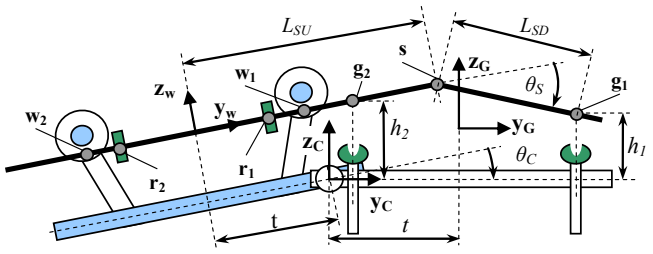

Fig. 6. Assembled LineScout Nomenclature

B. Analysis of the Geometric Constraints

The first step is to express wheel, roller and gripper locations on the wheel reference axis ($\mathbf{F_W}$) as:

$$\mathbf{w}_{1,2} = \begin{bmatrix} 0 \\ \pm E_W \\ 0 \end{bmatrix} \tag{1}$$

$$\mathbf{r}_{1,2} = \begin{bmatrix} 0 \\ \pm E_R \\ 0 \end{bmatrix} \tag{2}$$

$$\mathbf{g}_{1,2} = \begin{bmatrix} 0 \\ t + (t \pm E_G)\cos\theta_C + h_{1,2}\sin\theta_C \\ -L_C - (t \pm E_G)\sin\theta_C + h_{1,2}\cos\theta_C \end{bmatrix} \tag{3}$$

Then, the arm excursion h_1 and h_2 required to reach and grasp the conductor must be evaluated. If $\theta_S = 0$ or if both grippers close on the left side of point **s**, the third component of (3) is set to zero, giving:

$$-L_C - (t \pm E_G)\sin\theta_C + h_{1,2}\cos\theta_C = 0 \tag{4}$$

$$h_{1,2} = \frac{L_C + (t \pm E_G)\sin\theta_C}{\cos\theta_C} \tag{5}$$

If the above condition does not apply and $\mathbf{g_1}$ falls on the downward segment of the conductor, Fig. 6 and (6) are used to get an alternate $\mathbf{g_1}$ vector, called $\mathbf{g_1}^*$, calculated along the conductor's length:

$$\mathbf{g}_1^* = \begin{bmatrix} 0 \\ L_{SU} + L_{SD}\cos\theta_S \\ -L_{SD}\sin\theta_S \end{bmatrix} \tag{6}$$

And since $\mathbf{g_1}^*$ must equal $\mathbf{g_1}$ in (3), this gives:

$$g_{1y}^* = g_{1y} = L_{SU} + L_{SD}\cos\theta_S = t + (t + E_G)\cos\theta_C + h_1\sin\theta_C \tag{7}$$

and

$$g_{1z}^* = g_{1z} = L_C + (t + E_G)\sin\theta_C - h_1\cos\theta_C = L_{SD}\sin\theta_S \tag{8}$$

from (7), L_{SD} is isolated:

$$L_{SD} = \frac{(-L_{SU} + t + (t + E_G)\cos\theta_C + h_1\sin\theta_C)}{\cos\theta_S} \tag{9}$$

which is substituted in (8) to get h_1:

$$h_1 = \frac{L_C + (t + E_G)\sin\theta_C - \tan\theta_S\left[t(1 + \cos\theta_C) + E_G\cos\theta_C - L_{SU}\right]}{\tan\theta_S\sin\theta_C + \cos\theta_C} \tag{10}$$

From this last equation, it can be seen that the required excursion for h_1 not only depends upon the slope variation, θ_S, and the height of the platform, L_C, but also on the translation value, t, the rotation angle between the frames, θ_C, and the position at which the robot is stopped from the summit **s** prior to initiating the crossing, L_{SU}. Since these parameters depend on operator precision, the range of $h_{1,2}$ must be great enough to accommodate all situations.

By looking at Fig. 6, it becomes obvious that there is a range of values of t at which it is inappropriate to raise the grippers since they will collide either with the traction

wheels or the safety rollers located on the wheel frame. These critical locations also depend on the rotation value, θ_C, and are given by making either the **y**-components of $\mathbf{w}_{1,2}$ or $\mathbf{r}_{1,2}$ equal to the **y**-components of $\mathbf{g}_{1,2}$, from (1) to (3), into which (5) was incorporated in lieu of $h_{1,2}$.

$$t + (t \pm E_G)\cos\theta_C + L_C\tan\theta_C + (t \pm E_G)\sin\theta_C\tan\theta_C = \pm E_W \quad (11)$$

$$t = \frac{\pm E_W \mp E_G(1+\sin\theta_C\tan\theta_C) - L_C\tan\theta_C}{1+\cos\theta_C+\sin\theta_C\tan\theta_C} \quad (12)$$

The blue curves shown in Fig. 7 indicate the four possible values given by (12). The actual width of components is then considered by adding to or subtracting from their corresponding wheelbase half the values of D_W, D_R and D_G, and plotting new border curves in green on Fig. 7. Note that in the design actually chosen, the rollers are so close to the traction wheels that no usable space can be found between the two parts, implying that E_W-$D_W/2 \approx E_R$+$D_R/2$

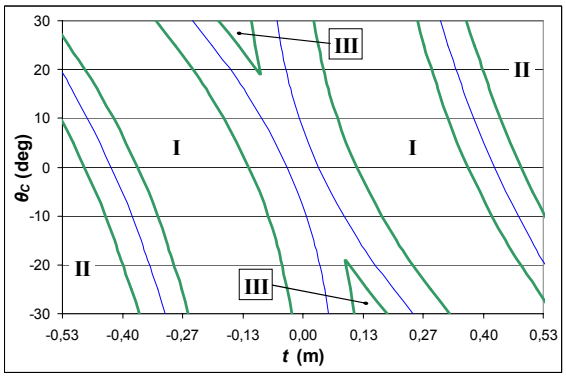

Fig. 7. Locations where the Grippers can grasp the conductor (I, II and III)

These results were critical not only at the design level to assess the validity of the chosen geometry but also later at the control level to protect the mechanical components by blocking the rise of the gripper arms except when located in the safe areas marked as I, II or III in Fig. 7.

C. Clearing Sequences

Two issues are now addressed, namely the longest obstacle that can be cross and how close the *subsequent* obstacle can be. Fig. 8 presents different clearing sequences possible with the LineScout on a straight section of conductors having a series of obstacles.

Each clearing sequence is characterized by the way the grippers are positioned around the obstacle being crossed, as illustrated by the four series of obstacles in Fig. 8. Depending on the length E_n of the nth obstacle being cleared (in blue), the following (or preceding) obstacle is schematized in grey as long and as close as possible.

Figure 8-1 shows the longest obstacle that it is possible to cross, thus the entire space between the two grippers is filled. In either direction, this normally requires that the adjacent obstacle be sufficiently far away to insert the two wheels *plus* one gripper (L_{n+2} or L_{n-2}). Actually, an obstacle can be located closer than this minimum distance, provided it is short enough to fit between the two rollers (E_{n+1} and E_{n-1}). In this case, the minimum distance to an adjacent obstacle is equal to the width of one gripper plus one wheel and a roller (L_{n+1} or L_{n-1}). The critical obstacle lengths are listed in Table 5 along with critical obstacle distances.

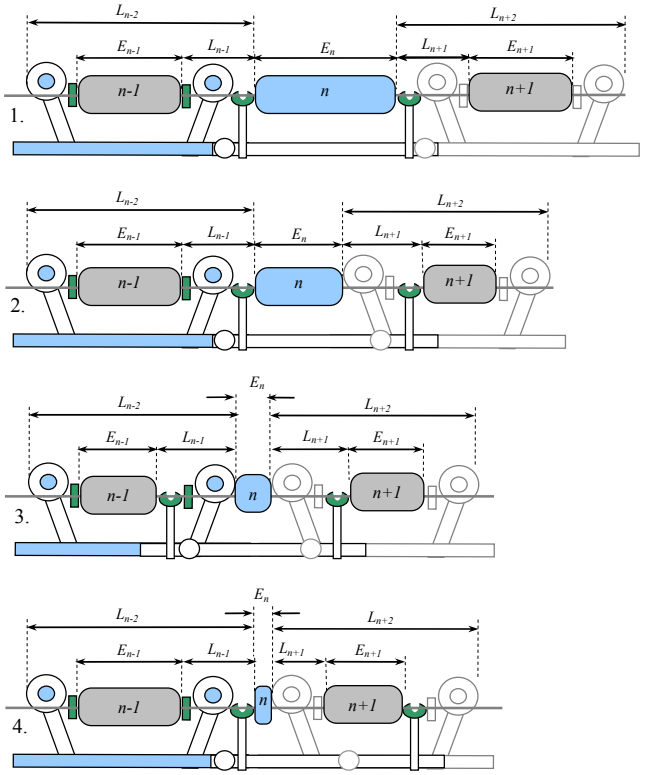

Fig. 8. Possible clearing sequence

While the left portion of Fig. 8-2 is identical to Fig. 8-1, the grasping arrangement differs on the right portion since the wheel and roller are inserted *between* the gripper and the n^{th} obstacle. The implications in terms of maximum obstacle lengths (E_n, $E_{n\pm1}$) and in terms of the minimum distance between obstacles ($L_{n\pm1}$, $L_{n\pm2}$) are listed in the second column of Table 5.

The clearing sequences described by Fig. 8-3 and 8-4 are appropriate for shorter obstacles and their geometric description is left to the reader, along with columns 3 and 4 of Table 5.

TABLE 5
CRITICAL OBSTACLE LENGTHS AND DISTANCES

	1	2	3	4
E_n	E_G - D_G	E_G-D_G-D_W-D_R	E_G-D_G-2D_R-2D_W	E_G+D_R-E_W
E_{n+1} E_{n-1}	E_W-D_W-2D_R	E_W-D_W-2D_R-D_G E_W-D_W-2D_R	E_W-D_W-2D_R-D_G	E_W-D_W-2D_R-D_G E_W-D_W-2D_R
L_{n+1} L_{n-1}	D_W+D_G+D_R	D_G+D_W+D_R	D_G+D_W+D_R	D_W+D_R D_G+D_W+D_R
L_{n+2} L_{n-2}	E_W+D_W+D_G	E_W+D_W D_G+E_W+D_W	E_W+D_W	E_W+D_W D_G+E_W+D_W

The expressions listed in Table 5 were evaluated by using the actual geometric parameters of the LineScout and plotted

on Fig. 9 to graphically assess the actual clearing capacity of the vehicle. The green circular dots represent a sample of identified obstacles that must be cleared, located by their known length and typical installation distance range (indicated by a vertical green line).

The vertical red line at 0.84 m is the absolute maximum crossable length and the stepped horizontal red line represents the different values of $L_{n\pm2}$. Therefore, the area marked as A covers obstacles that are crossable regardless of the length of the next obstacle.

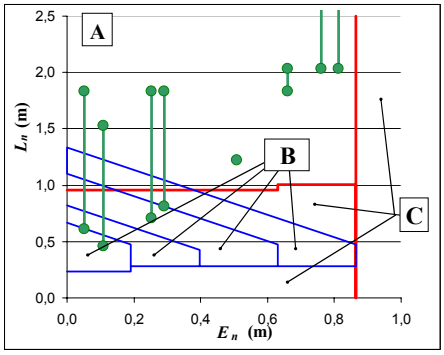

Fig. 9. Envelope of the clearing sequence

The areas marked as B cover obstacles that are crossable provided that a specific distance-to-length relationship is maintained. The lower limit of this area is given by the values of $L_{n\pm1}$ as per Table 5. The higher (diagonal) limit for each clearing sequence is drawn assuming that next obstacle is 0.30 m long. Since this is slightly less than $E_{n\pm1}$ and if the obstacle is also shorter than E_n, a margin appears that is added to the minimal distance $L_{n\pm1}$ evaluated by Table 5. Areas marked as C are therefore impossible to cross as the obstacle is either too long, too closes from one another or an inappropriate combination of both. As can be concluded from Fig. 9, all green dots fall in a crossable area.

V. Prototype Design

Geometric analysis, as presented in the previous section, was used extensively at an early stage to validate the design of the first working LineScout prototype. After a few iterations and mechanical adjustments, the final prototype shown in Fig. 10 was assembled.

This prototype is built from extruded aluminum sections, standard purchased modules and machined parts. It contains 11 motors remotely-controlled by PWM amplifiers. Crossing an obstacle with the LineScout takes an experienced operator about two minutes. The prototype was thoroughly validated and successfully tested on the Hydro-Québec network on live lines at 315 kV (Fig. 11), and up to 735 kV. The following section presents a variety of particularly innovative aspects of the LineScout mechanical design.

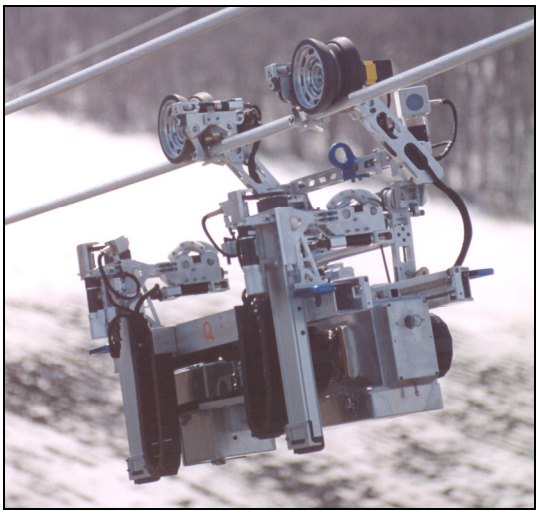
Fig. 10. LineScout prototype climbing a bundled conductor

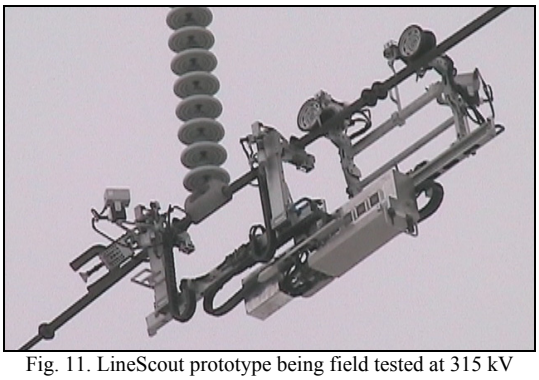
Fig. 11. LineScout prototype being field tested at 315 kV

A. Traction Wheels

On Fig. 12, a 300 W brushless DC motor (1) coupled to a planetary flanged-output gearbox (2) with built-in heavy-duty cross-roller bearing directly supports the wheel, assembled by tightening a set of light plates (4) that compress a molded part of natural conductive rubber (5) and an adjustment shim (6).

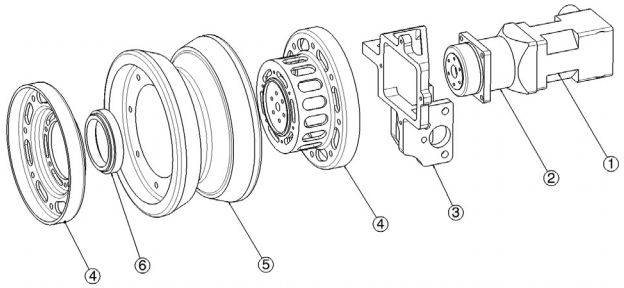

Fig. 12. LineScout traction wheel design

B. Grippers and Safety Rollers

These simple but critical systems share the same principle (Fig. 13). Both use a right-end and left-end single-thread worm shaft (1) with matched worm gears (2) and take advantage of the self-locking characteristic of such an

assembly. To ensure against unwanted opening of the rollers or grippers, movement of the drive shaft is monitored by an absolute potentiometer, coupled to the DC motor (3) that transfers the motion via a pair of spur gears (4). The contact elements are covered by a protective sleeve of conductive nylon (5).

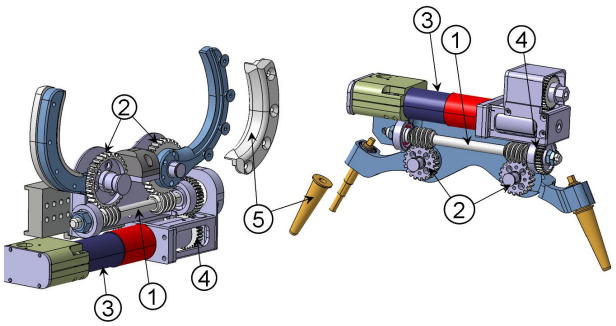

Fig. 13. LineScout gripper and roller design

C. Center Frame

The Center Frame is the heart of the LineScout, supporting 40% of the total weight while generating both the translational and rotational degrees of freedom. As seen in Fig. 14, two machined plates (1 and 2) are mounted on a set of concentric shafts (3 and 4) and can be rotated by means of a sector of worm gear (5) actuated by a DC motor (6). A third concentric shaft (7) goes from one side to the other and is rotated by a second motor mounted underneath (8). This shaft, with sprockets on either end, can simultaneously drive two roller chains (9). One chain is attached to the wheel frame (10), the other to the gripper frame (11). Since there are two pairs of idler rollers on one side and one pair on the other side, the chains mesh on different sides of the sprockets so translations occur in opposite directions.

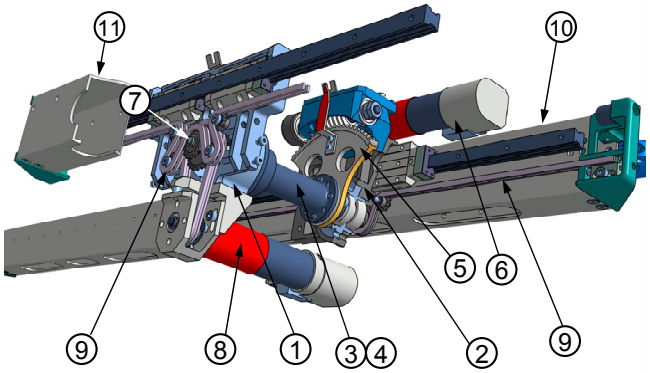

Fig. 14. LineScout Center Frame design

D. Deployment Arms

This degree of freedom enables the upper wheel assembly to fold down once the platform is suspended by the grippers and the traction wheels are slightly, as illustrated by upper part of Fig. 15. This movement requires roughly 28 Nm of torque at the bottom drive shaft while the same axis of movement must sustain almost six times that torque (168 Nm) when the entire weight of the vehicle sits on the wheels.

To help reduce the size of the motor and gearbox for this axis, a disconnecting mechanism was introduced so that none of the second (and higher) torque is transferred to the actuation tube. The lower portion of Fig. 15 is a close-up view of the disconnecting mechanisms.

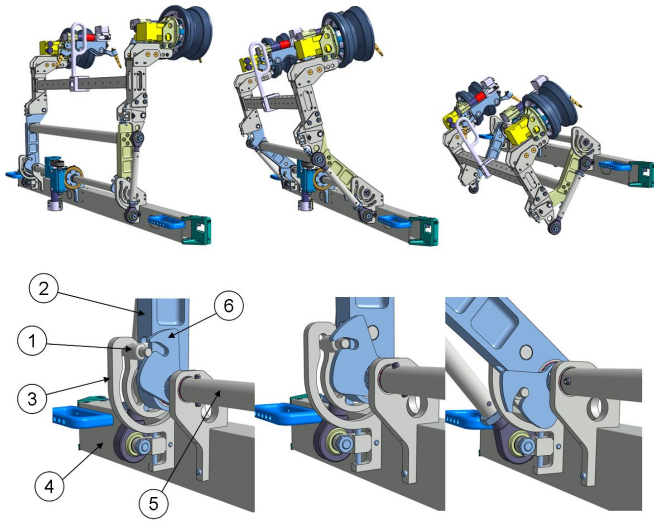

Fig. 15.LineScout flipping arm design

A pivoting link supporting a lateral pin (1) is attached to the vertical arm (2) and is inserted into a grooved plate (3) attached to the wheel frame (4). When the link is up into the end portion of the groove, the vertical arm is locked with respect to the wheel frame. Since the actuation tube (5) terminates in notched plates (6), as it rotates, it brings the link out of the end groove down to a circular portion of the grooved plate and the vertical arm is then released with respect to the wheel frame and locked with respect to the motorized actuation tube.

E. Battery consumption and gauges

The LineScout's source of energy is a high-power Li-ion battery. Table 6 summarizes power needs for the different tasks performed based on initial testing of the prototype. Energy consumption is for a typical 6-hour of work day.

TABLE 6
TYPICAL POWER AND ENERGY CONSUMPTION

LineScout Task	Duration (% of day)	Power (W)	Energy (Wh)
Sleep mode	10%	14	8
Stand-by and inspection	30%	90	162
Crossing an obstacle	15%	150	135
Climbing 5 deg @ 0.75 m/sec	40%	225	540
Climbing 15 deg @ 0.6 m/sec	4%	350	84
Climbing 25 deg @ 0.3 m/sec	1%	400	24
Typical day consumption			863

A battery pack consisting of 4 commercially available 24-VDC Li-ion batteries was assembled to provide a nominal voltage of 48 VDC. When fully charged, it contains 1080 Wh of energy at a maximum voltage of 57.6 VDC. Real-

time battery voltage is transmitted to the operator on the ground, who estimates the remaining autonomy of the LineScout, based discharge experimental data, as plotted in Fig. 16. Since the measured voltage (in blue) fluctuates as the power demand varies, the estimated energy level (in green) must be filtered out (in red), mainly to eliminate the voltage *peaks* generated when descending steep slopes. Recharging the battery with these descents and integrating the battery current to provide a better consumption estimates were considered but discarded so far due to added complexity.

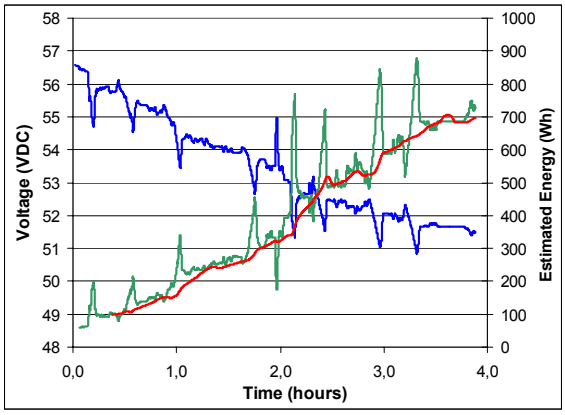

Fig. 16. Battery voltage drop and estimated discharge rate

VI. Future Development and Conclusion

A mobile robotic platform for transmission line inspection and maintenance, called the LineScout, has been presented. The third-generation prototype has been tested and validated under field conditions. The introduction of the LineScout into a previously robotic-free field of application was made possible by taking into consideration the end-users perspectives and by systematically analyse the geometry in order to appropriately customize its dimensions. Various other aspects of the technology, like teleoperation control, design and ergonomics of the operator interface, design and validation of inspection modules, and electronic design for very-high voltage EMI shielding will be covered in future publications.

Everything is now in place to make the LineScout technology grow into an autonomous vehicle. In the future, the same type of analysis and added sensors could be used to allow the LineScout to autonomously select the appropriate clearing sequence, as it would then be able to identify the position and size of upcoming obstacles.

Acknowledgment

The authors would like to personally thank all the development team members of the *Institut de Recherche d'Hydro-Québec (IREQ)*. Thanks to Hydro-Québec TransÉnergie personnel for their precious collaboration in this innovative and challenging project.

References

[1] Montambault, S. and Pouliot. N., 2004, "On the Economic and Strategic Impact of Robotics Applied to Transmission Line Maintenance", 7th International Conference on Live Maintenance (ICOLIM 2004), Bucharest, Romania.

[2] Jiang, B. and Mamishev, V., 2004, "Robotic monitoring of power systems", IEEE Transactions on Power Delivery, Vol. 19, No. 3, July, 2004.

[3] Ruaux, P., 1995, "Mechanization of the Installation of Aircraft Warning Spheres on Overhead Lines", Proceedings of the 1995 International Conference on Transmission and Distribution Construction, Operation and Live-Line Maintenance, pp. 125-131.

[4] Campos, M.F.M., Pereira, G.A.S., Vale, S.R.C., Bracarense, A.Q., Pinheiro, G.A., Oliveira, M.P., 2002, "A Mobile Manipulator for Installation and Removal of Aircraft Warning Spheres on Aerial Power Transmission Lines", Proceedings of the 2002 IEEE International Conference on Robotics and Automation. May 11-15, Washington, DC.

[5] Earp, G., 1997, "EA Technology's Robotics Program", Proceedings of Robotics for Use in the Electricity Industry, Feb. 4, 1997, Capenhurst, England.

[6] Rochia, J. and Sequeira, J., 2004, "The development of a robotic system for maintenance and inspection of power lines", Proceedings of the 35th International Symposium on Robotics, Paris.

[7] Zhou, F.Y., Wang, J.D., Li, Y.B., Wang, J. and Xiao, H.R., 2005, "Control of an inspection robot for 110 kV power transmission lines based on expert system design methods", Proceedings of the 2005 IEEE Conference on Control Applications, Toronto, Canada.

[8] Sawada, J. et al., 1991 "A Mobile Robot for Inspection of Power Transmission Lines", 1991, IEEE Transactions on Power Delivery, Vol.6, No.1, pp. 309-315.

[9] Xiao, X.H., Wu, G., and Li, S., 2007, "Dynamic Coupling Simulation of a Power Transmission Line Inspection Robot with its Flexible Moving Path when Overcoming Obstacles", 3rd Annula IEEE Conference on Automation Science and Engineering, Sept. 22-25 2007, Scottsdale, AZ, USA

[10] Montambault, S. and Pouliot, N., 2003, "The HQ LineROVer: Contributing to Innovation in Transmission Line Maintenance", 10th International Conference on Transmission and Distribution Construction, Operation and Live-Line Maintenance (ESMO 2003), April 6-10, Orlando, Florida.

[11] Montambault, S. and Pouliot, N., 2006, "LineScout Technology: Development of an Inspection Robot Capable of Clearing Obstacles While Operating on a Live Line", 11th International Conference on Transmission and Distribution Construction, Operation and Live-Line Maintenance (ESMO 2006), Oct. 15-18, Albuquerque, New-Mexico.

[12] Montambault, S. and Pouliot, N., 2007, "Design and Validation of a Mobile Robot for Power Line Inspection and Maintenance", Proceedings of The 6th International Conference on Field and Service Robotics, July 9-12 2007, Chamonix Mont-Blanc, France.